CANADIAN JOURNAL OF EXPLORATION GEOPHYSICS
VOL. 30, NO 2 (DECEMBER 1994), P 84-92

A STRUCTURAL MODEL OF A GRABEN BOUNDARY FAULT SYSTEM, SIRTE BASIN, LIBYA: COMPACTION STRUCTURES AND TRANSFER ZONES[1]

ANDREW G. SKUCE[2]

ABSTRACT

The Agedabia Trough is the deepest of the several rift-derived subbasins that form the Sirte Basin in Libya. The SW boundary of this trough is defined by a system of large normal faults. These faults are interpreted to be mostly planar, basement-involved fault segments linked together by transfer zones. The nature of the displacement transfer varies with depth within these zones. The small-scale structural details within the zones are obscure but some characteristics can be inferred by comparison with structural models from other settings.

The synrift and postrift sediments in the hanging walls of the large faults typically show monoclinal structures dipping into the trough. These structures are interpreted to have been generated through compaction of the sediments over the fault step in the basement. Computed forward models illustrate that compaction and sedimentary growth across the fault zone is sufficient to produce structures similar in geometry and magnitude to the observed features. Other mechanisms, such as fault-bend folding, did not significantly contribute to the development of the structures. The model also shows that compaction can cause sedimentary growth to occur within the hanging wall rather than just at the fault plane. In certain circumstances, anticlines in the hanging wall can also form as a sole result of compaction. Generally, compaction is one of the most important mechanisms in the deformation of normal fault hanging walls, even in areas where basement is not involved in the faulting.

INTRODUCTION

Since the early 1980s structural modelling of extensional fault geometries has become an essential tool for constraining and guiding interpretations in areas of complex structure or limited data. In most extensional basins with proven hydrocarbon potential, the obvious large four-way anticlinal closures and footwall fault traps have long been drilled and the explorer is faced with finding prospects which are typically either small, complex or in poor data areas. Untested structures are more likely to be deep rather than shallow and in the hanging walls rather than the footwalls of normal faults. It is the main purpose of this paper to show that compaction of sediments is a principal cause of oil-field scale structures in the hanging walls of normal faults. (For want of a better term, 'oil-field scale' here means a structure having amplitudes of the order of hundreds of metres and wavelengths of the order of kilometres.) Modelling of such compaction structures should lead to a better understanding of the development of the structures as well as the age, geometry and the nature of the rocks involved. Compaction structures in the hanging walls of normal faults sometimes termed 'lick-up' (Graham, 1992) have previously been recognized in the North Sea (e.g., Evans and Parkinson, 1983; White et al., 1986; Badley et al., 1988; Milton et al., 1990) and in the Cooper Basin of Australia (Gray and Roberts, 1984).

The Sirte Basin of Libya (Figure 1) was formed by lithospheric extension that began in the Late Cretaceous, followed by thermal subsidence which lasted from the Maastrichtian onwards (Gumati and Nairn, 1991). A lesser phase of rifting occurred in the Eocene, reactivating the older normal faults. The Sirte Basin comprises a number of platforms and subbasins.

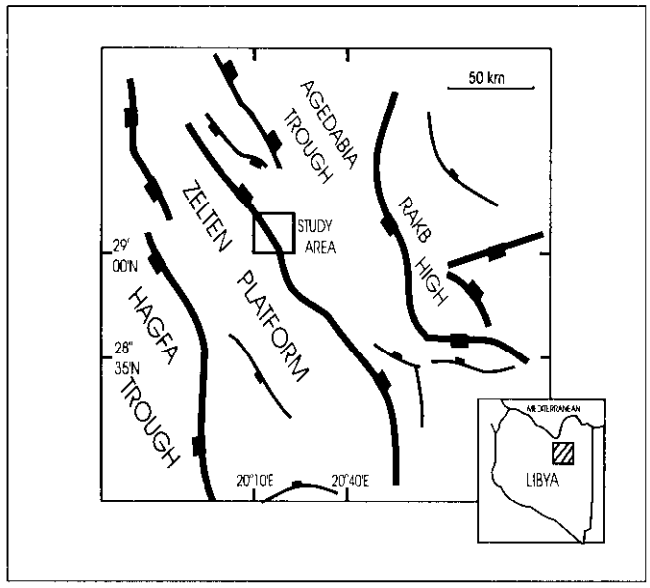

Fig. 1. Location of the Agedabia Trough and the Zelten Platform in the Sirte Basin of Libya.

[1]Presented at the CSEG/CSPG Joint Convention, Calgary, Alberta, May 10, 1994. Manuscript received by the Editor September 9, 1994; revised manuscript received December 13, 1994.

[2]Husky Oil Operations Ltd., Box 6525, Station D, Calgary, Alberta T2P 3G7

The author would like to acknowledge the managements of the National Oil Company of Libya, OMV and Husky Oil International for kindly granting permission to publish this paper. Peter Buchanan of Cogniseis performed the GEOSEC modelling and made many useful suggestions. Colleagues Darrell Keiver, Hugh Wishart and Franz Schmidt assisted with the geology. Michael Enachescu and three anonymous reviewers suggested several improvements to the manuscript. Maria Nemethy and Shannon Wahler prepared the figures.

The deepest of the subbasins is the Agedabia (or Sirte) Trough which contains Upper Cretaceous and Tertiary sediments more than 6 km thick. At the time of writing, no well has yet penetrated the complete sedimentary section within the trough. The study area (Figure 1) straddles the fault zone that marks the boundary between the Agedabia Trough and the Zelten Platform.

Figure 2 summarizes the formation names and lithologies of the major units in the study area. The lower parts of the Rakb and the Etel Formations are not present on the Zelten Platform. The most economically significant reservoir units in the area are the prerift Nubian Sandstones (Clifford et al., 1980) of the Sarir Formation that lie directly on the basement and the pinnacle reefs and platform carbonates of the Sabil Formation (Terry and Williams, 1969). Giant oil fields in the area consist either of large structural closures on the platforms or stratigraphically trapped Upper Sabil reefs within the Agedabia Trough.

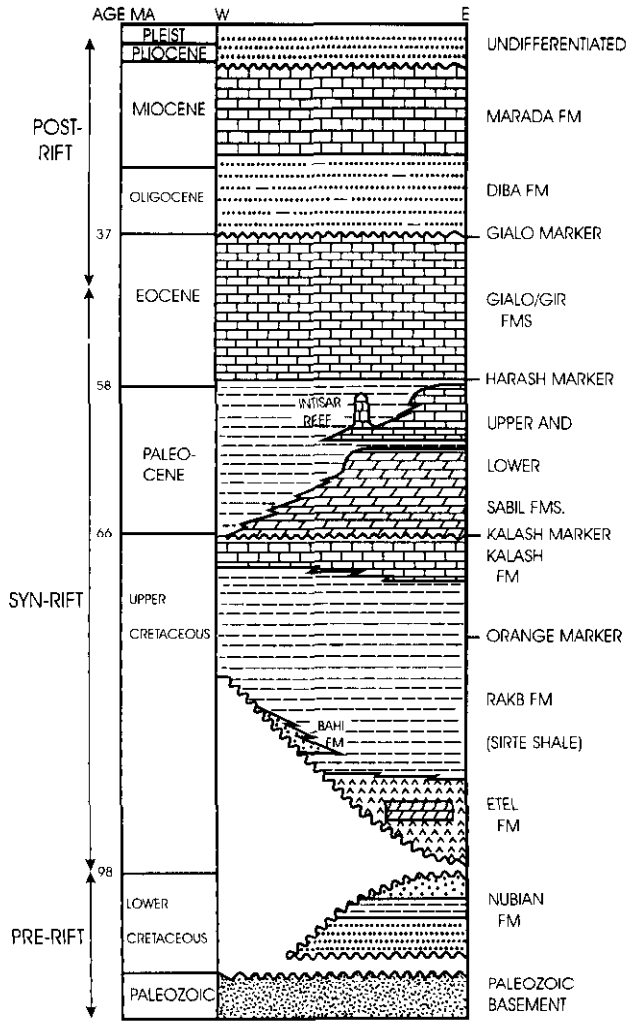

Fig. 2. Generalized stratigraphic column for the study area. The lower part of the Rakb Fm and the Etel Fm are not present on the Zelten Platform. No wells in the area have penetrated units older than the Orange horizon in the Agedabia Trough in the immediate area, so the deep geology is extrapolated from further away.

Structure

Figure 3 shows an interpreted time-migrated seismic line over the normal fault which separates the Agedabia Trough from the Zelten Platform. Two nearby wells have been projected a few hundred metres onto the line. These control the identification of seismic markers down to the top Kalash horizon within the trough and the top Bahi horizon on the platform. Basement was penetrated in neither well, but other nearby wells on the Zelten Platform have reached basement and allow the picking of the top basement horizon on the platform. The basement top typically produces a weak seismic response in this part of Libya and its interpretation often has to be ghosted in. A deep well within the trough, some 20 km to the east, penetrated about 800 m into the Rakb Formation. The 'Orange' horizon is observed just below the base of this well and has been tentatively correlated to the top of the Campanian. The time section was converted to depth (Figure 4) using velocities derived from sonic logs in nearby wells and extrapolated below the 'Orange' horizon. Inverse image ray modelling, using the program '2D-AIMS', was performed to remove any depth migration effects which were, in any case, slight.

The position of the normal fault is defined in the upper and middle parts of the section by reflection terminations of the horizons in the footwall and hanging wall; however, its deeper geometry is not clear. The NE-dipping reflectors at depth, below the Orange horizon, are thought to be partly real structural dips, but where these reflectors occur in the footwall of the fault they are interpreted as wavefront artifacts produced by the migration. The fault is mostly planar, but a slight fault bend has been interpreted around 2 seconds. Depth conversion tends to reduce the apparent amount of listric fault curvature observed on time sections since average velocities generally increase with depth. Some horizons show slight rollover into the fault and a minor antithetic fault is observed.

Apart from the normal fault itself, the most significant structure on the section is the monocline seen in all nonbasement reflectors in the hanging wall of the fault. The structure dips to the NE, away from the fault, and is bounded to the SW and NE, respectively, by anticlinal and synclinal fold axes. Two characteristics of this monocline are important: (1) the steepness of the monocline is greater on deeper horizons, 10° at the Harash, 18° at the Kalash and 21° at the Orange; (2) the axial plane of the syncline that defines the NE limit of the monocline is approximately vertical.

Consideration of these two factors led to the interpretation of the monocline as a compaction structure over the basement fault block. Generally, one would expect compaction effects to increase with depth. The process of compaction is driven by gravity; in the absence of other forces, any particle displacement should therefore be straight downwards. Any deformation due to differential vertical movements can be modelled by vertical simple shear. Therefore, any folding induced by compaction would be expected to have vertical axial planes.

If a planar geometry for the deeper part of the fault is assumed, then the top basement depth within the trough can be readily estimated as lying at the intersection of the downward projection of the fault plane and the synclinal axial plane of the compaction fold. 'Basement', for these purposes, would include any noncompactable or precompacted sediments such as the prerift Sarir Sandstones. Obviously, any such estimate is going to be crude, but it has the advantage that it can be made quickly and simply on a seismic time section (if the velocities do not change abruptly) and is likely to be as good as or better than estimates made from other geophysical techniques such as gravity or magnetics in areas where there is no direct control (seismic or well data) of basement depths. Map views of the fault system (Figure 5) show that, for the most part, the monoclines that developed in the hanging wall lie approximately vertically above each other and are coincident with the interpreted basement fault heaves.

Along strike to the NW, the expression of the normal fault becomes more complex, the fault divides into two or more splays and, in places, rollovers of some of the shallow hanging wall horizons indicate that the fault is not always strictly planar. Two small transfer zones have been interpreted (Figures 5, 6). The details within the transfer zones cannot be fully imaged with the available two-dimensional seismic coverage and the basement structure is conjectural since it is

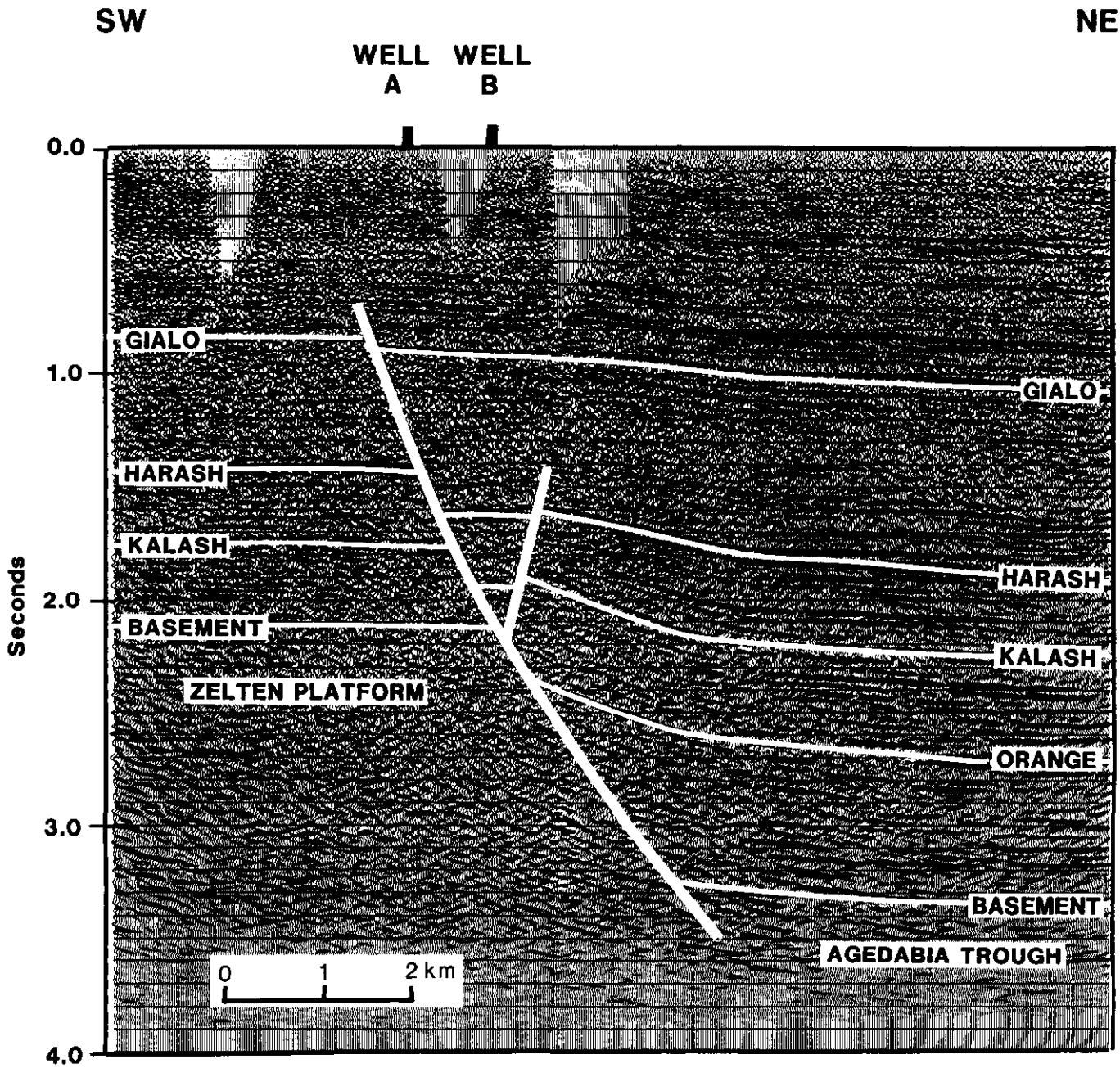

Fig. 3. Migrated Vibroseis line across the fault that separates the Zelten Platform from the Agedabia Trough. The line is located in the southern part of the study area outlined in Figure 1.

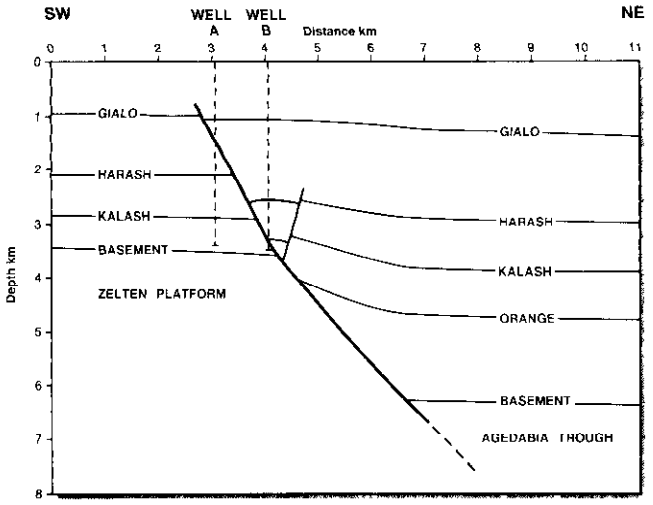

Fig. 4. Depth-converted interpretation of data in Figure 3.

based largely on the structural model described above. Seismic sections that run across the transfer zones are difficult to interpret since they are contaminated with energy from out of the plane of the section. Three-dimensional seismic data are required to properly image these features. The transfer zones are similar to the model proposed by Peacock and Sanderson (1994) (compare their figure 12 with my Figure 6). At the level of the Gialo horizon (not shown) the normal fault traces do not overlap at the transfer zone; Morley et al. (1990) would classify this kind of transfer zone as 'approaching', whereas the map view pattern at the deeper horizons (Harash, Kalash) would be classified by them as 'overlapping'. At deeper levels still, the faults are inferred to be hard-linked by transfer faults. Peacock and Sanderson (1994) noted that the different character of the transfer zones with depth reflects the development of the zones as fault displacement increases and the originally independent faults extend laterally, eventually starting to interact. Thus, the shallowest horizons, where the fault displacements are smallest, have a geometry that probably resembled the geometry of transfer zones at deeper horizons at an earlier stage of the rifting.

Studies of the distribution of strain in normal fault zones show that extension is predominantly effected on the largest faults except within transfer zones where smaller faults, mostly below the limits of seismic resolution, take up a larger proportion of the extension (Childs et al., 1994; Morley, 1994). Within transfer zones, the relay ramp will be subject to torsion, causing the orientations of the faults and fractures to be variable (Peacock and Sanderson, 1994). Because segments of permeable horizons are less likely to be isolated by fault offsets and because fracturing is likely to be more intense, transfer zones are prone to being areas of enhanced permeability compared with the larger, simpler faults between the transfer zones. At shallower levels, relay ramps will connect the same horizon in the footwall and hanging wall directly, without any faulting. Thus, transfer zones will provide hydrocarbon migration pathways, which is beneficial for the charging of footwall traps but detrimental for the seals of hanging wall traps that involve a transfer zone. D. Klepacki (personal communication) has pointed out that some of the overthrust traps in the Foothills of the Canadian Rockies are not full to their structural spill point and that leakage seems to occur at compressional transfer zones, where one would also expect a higher density of smaller faults and fractures with variable orientations.

Figure 6 can be contrasted with figure 4 of Morley et al. (1990). Their models of transfer zones in rifts involve listric faults with strong anticlinal rollovers in their hanging walls. Certain seismological studies of currently active normal faults show that these faults are approximately planar and typically have dips in the range of 45-65° (Jackson, 1987; Westaway and Kusznir, 1993). Kusznir et al. (1991) show that basin models using essentially planar faults account for the subsidence history and geometry of certain rift basins better than models that assume listric faults. Rollover of both basement and the sedimentary horizons is a necessary geometric consequence of listric faulting but is not observed in the case described in this paper. The models of Morley et al. (1990) are appropriate for linked fault systems in areas of detached faulting, such as deltas. In rifted areas large normal faults involving basement are more likely to be subplanar features which terminate downwards in the ductile lower crust.

A Forward Model

When the interpretation of compaction structures was first made, it was not clear as to whether or not it was quantitatively reasonable. Specifically, it was uncertain whether compaction alone was sufficient to produce features of the magnitude and geometry observed in the data and, if not, what additional mechanisms would have to be invoked to explain the origin of the structures. Accordingly, a forward model (Figure 7) was produced using the GEOSEC software. The purpose of this model was to determine the form and the order of magnitude of compaction structures, given a set of quantitative assumptions about the structural and sedimentary history of the part of the Sirte Basin examined in this paper. No attempt was made to produce an exact match between model and example.

Within the modelling program, compaction occurs according to the thickness of sediments directly above the layer at a particular point. Porosities do not vary with depth for any particular vertical column within a layer and a layer does not compact under its own weight. These assumptions may produce modelling artifacts that could be reduced by making the layers thinner. The compaction profile selected for the shale units was the Baldwin-Butler (1985) relationship. The maximum permitted porosity of shales within the program (i.e., at zero depth) is limited to 45%. This means that a fully compacted (i.e., zero porosity) shale at depth will have a bed thickness that is 55% of its original thickness when deposited. Mixed lithologies compact at rates proportionally between the rates for the pure lithologies. Sands compact according to the Sclater-Christie curve and carbonates according to the Schmoker-Hailey relationship, as described in Baldwin and Butler (1985).

The development of the model at each stage is shown in Figure 7. The first compaction structures appear at stage 4. In stage 5, unit c is deposited as a thicker unit in the hanging wall than the footwall due to compaction subsidence of unit a. Note that the thickening of unit c occurs above the hanging wall and not as growth across the fault plane. Stages 6 and 7 show the effects of further compaction, subsidence and deposition. For the first time, in stage 8, compaction occurs in the footwall. The fault moves again in stage 9, cutting through and displacing units c and d, followed by the deposition of unit e.

Note that unit e thickens both at the fault plane and within the hanging wall due to compaction of lower units. The fault in the shallower section in stage 9 is assumed to have the same dip as its continuation below where it offsets the basement. At stage 10, compaction has resulted in the upper part of the fault rotating, producing a convex fault bend at the footwall cutoff of the basement horizon. Continued movement on the fault (not modelled) would result in fault-bend folding in the units above the bend.

The top of unit e in stage 10 has formed an anticline. This feature is, in part, an artifact resulting from the thinning by faulting of unit d before compaction. The use of thinner intervals with intermediate compaction stages for unit e would diminish this effect. Nevertheless, there could be geological

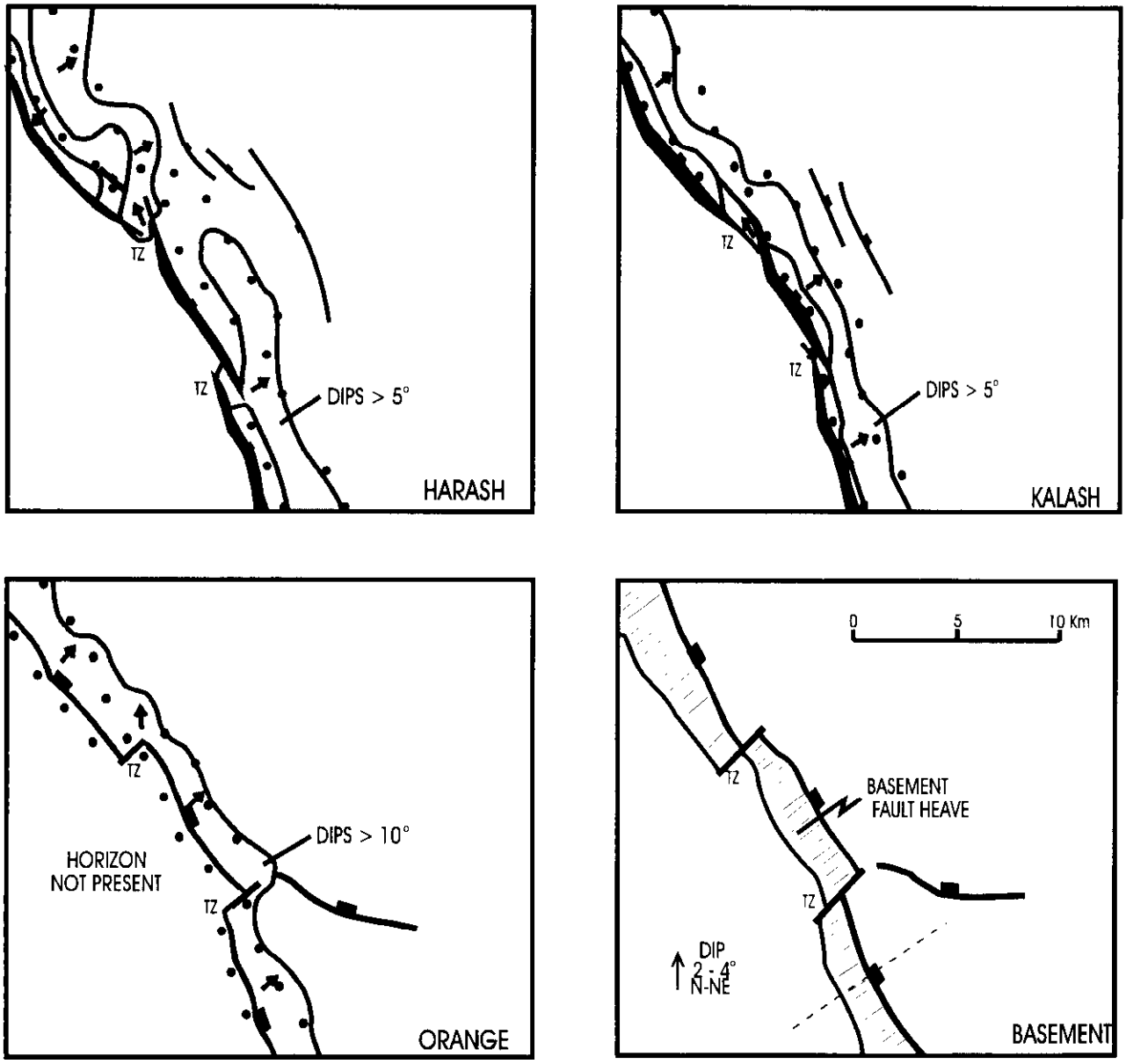

Fig. 5. Map views of some of the horizons interpreted in Figures 3 and 4. Fault heaves for the Harash and Kalash horizons are shown in black; basement fault heaves are shown with a diagonally shaded ornament; the Orange horizon is not present in the footwall, so only its hanging wall cutoff is shown. The shaded areas mark the extent of steeper than regional basinward (NE) dips for the three nonbasement horizons. Note the coincidence between these areas and the basement fault heave (dotted lines). Note also that the faults at the Harash and Kalash levels overlap at the transfer zones, whereas the deeper two horizons do not. The area shown is the small rectangle in Figure 1. The antithetic fault shown in Figures 3 and 4 is omitted for clarity. The dashed line on the basement level map shows the approximate position of the seismic line (Figure 3).

circumstances where an anticline could develop as a result of compaction in the hanging wall of a fault, as shown in the model. The final two stages of the model show the deposition of unit f and the continued compaction of the deeper units.

Comparison of the model with the actual depth interpretation (Figure 5) shows that many of the features of the model match the data quite well, especially the vertical nature of the synclinal fold axis and its location immediately above the hanging wall cutoff of the basement. The anticlinal axis of the fold is not vertical and is not related in a simple way to the footwall cutoff of the basement. The units c, d, e and f are all thicker in the basin than over the platform, but only unit e thickens at the fault plane; the rest of the thickening occurs in the hanging wall of the fault above the basement fault heave. Such effects are also clearly seen in the data. Thus, sedimentary growth across a fault, as seen between two wells, need not occur in its entirety at the fault plane, as it might be interpreted on geological sections in the absence of seismic data.

The magnitude of the dips of the compaction structures (30°) is considerably greater on the models than is observed in the data (21°) at the level of the deeper horizons. A possible reason for this is the unknown lithologies of the deeper units; these could consist of rock types less compactable than the Baldwin-Butler shales chosen in the model. Alternatively, the deeper units could be composed of relatively under-compacted shales, which also would mean that the model has overestimated the amount of compaction.

A further mismatch between the model and the data can be seen by comparing the shape of the Harash reflection in the immediate hanging wall of the fault in Figure 4 with the top of unit d in stage 12 of Figure 7. In the data, the horizon rolls over, dipping very slightly to the SW, whereas in the model the horizon dips to the NE. The rollover could be due to folding above a slight concave bend in the fault (referred to above) but this effect was not modelled. A model which combines fault-bend folding and compaction is likely to be complex since more than one deformation mechanism is

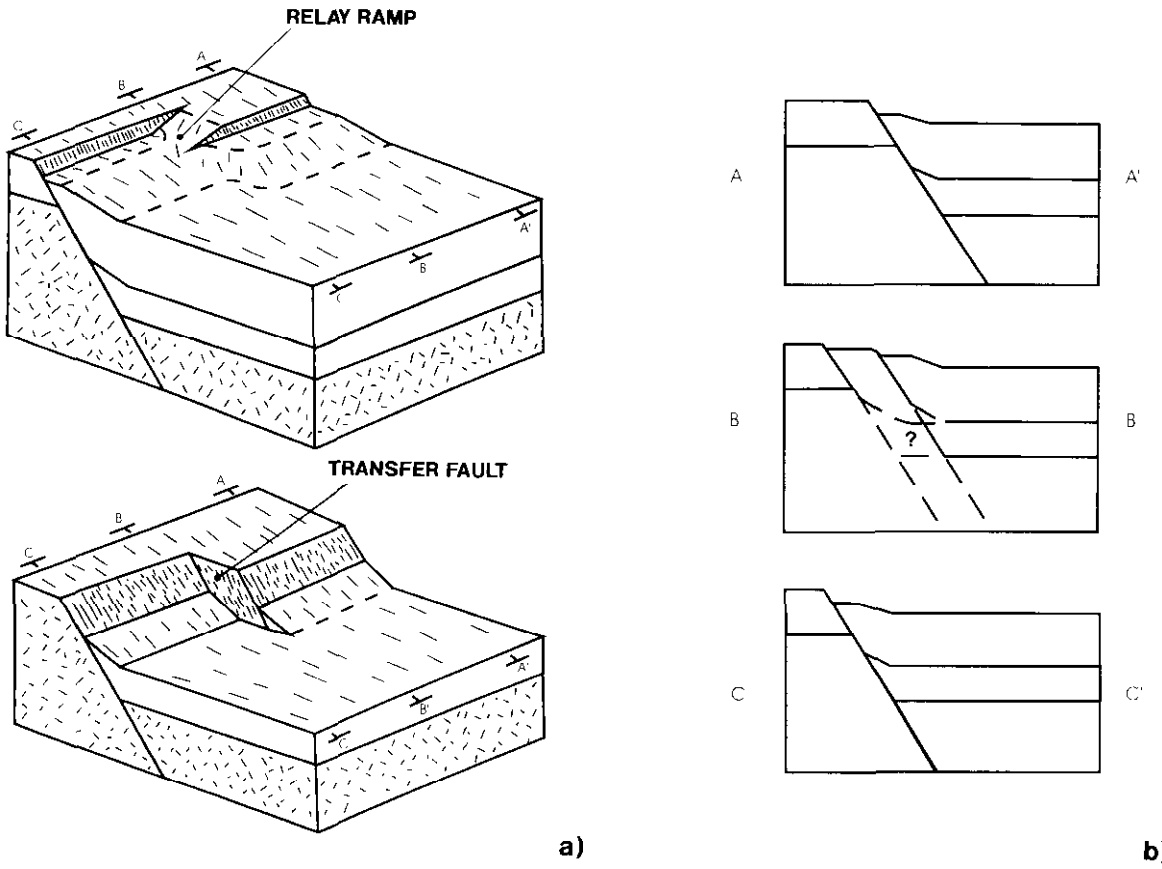

Fig. 6. Diagrammatic views of **(a)** and 'seismic' sections across **(b)** a normal fault and transfer zone. Section B, which runs above the transfer zone, will be contaminated with out of the plane energy and will be difficult to interpret. Note how the transfer zone changes in style with depth and how the compaction monoclines and relay structures interact.

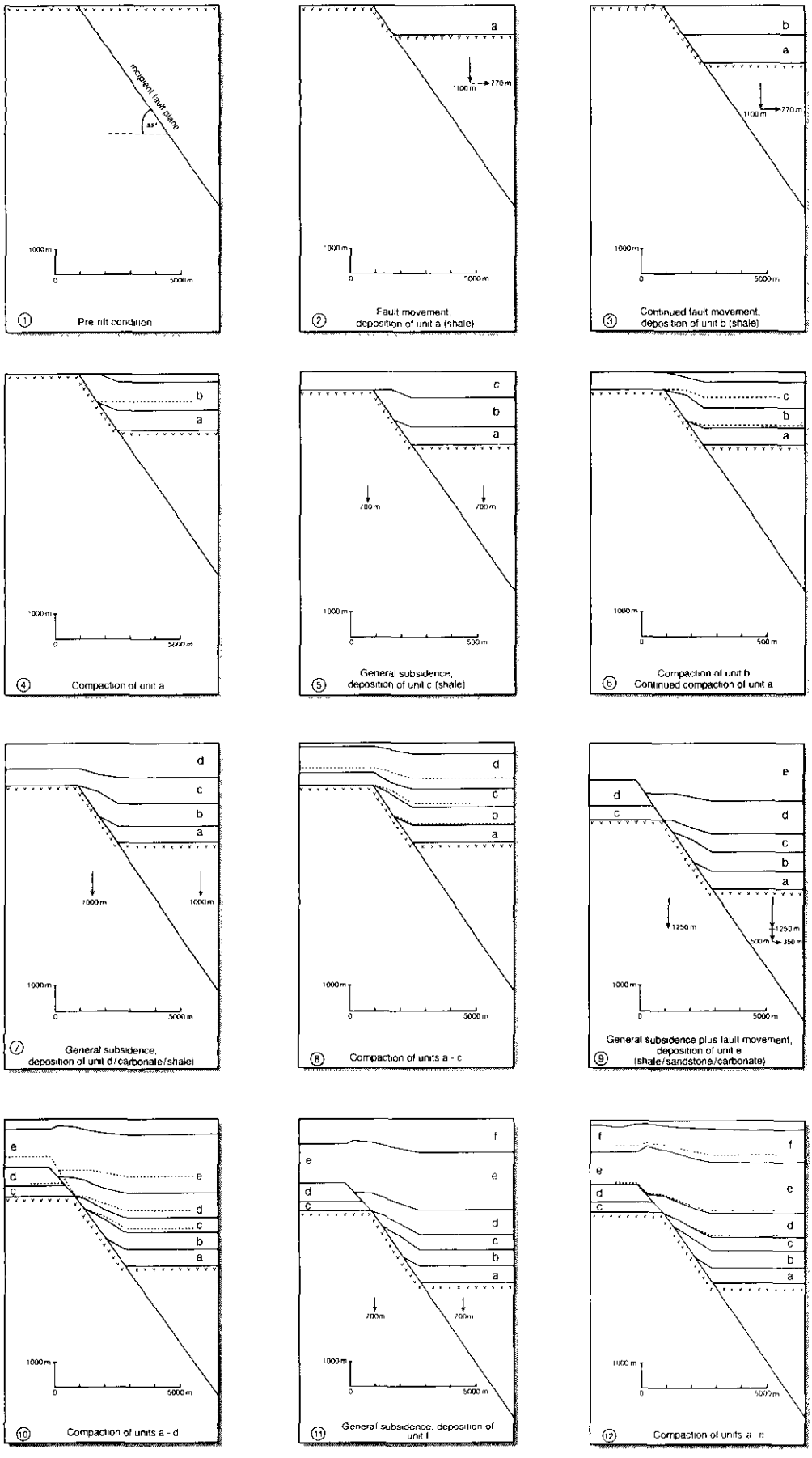
incipient fault plane
55°
1000 m
0
5000 m
① Pre rift condition
a
100 m
770 m
② Fault movement, deposition of unit a (shale)
b
a
1100 m
770 m
③ Continued fault movement, deposition of unit b (shale)
④ Compaction of unit a
c
700 m
500 m
⑤ General subsidence, deposition of unit c (shale)
⑥ Compaction of unit b Continued compaction of unit a
d
1000 m
⑦ General subsidence, deposition of unit d / carbonate / shale)
⑧ Compaction of units a - c
e
1250 m
500 m
350 m
General subsidence plus fault movement, deposition of unit e (shale / sandstone / carbonate)
⑩ Compaction of units a - d
f
⑪ General subsidence, deposition of unit f
⑫ Compaction of units a - e

active simultaneously. Here, compaction is assumed to be accommodated by normal simple shear, whereas rollover structures are best modelled by using antithetically inclined simple shear (White et al., 1986; Xiao and Suppe, 1992).

The reduced dip of the upper part of the fault plane predicted in the model is not observed in the data. As noted above, the assumption in the model was that the original dip of the fault plane in the upper section before compaction (stage 9) was the same as that in the deeper section. If it had been assumed that the original fault dip in the shallow section was around 62°, then after compaction the dip of the fault would have been about the same as in the deeper section.

Despite the limitations mentioned above, the model shown here does allow the following conclusion: oil-field scale structures can be formed by compaction of sediments above a normal fault. As a consequence of their geometry, these structures require a seal against the fault in order to form suitable hydrocarbon traps.

Discussion

There are several other mechanisms capable of producing basinward (or synthetic) dips in the hanging walls of normal faults, for example: a) frictional drag along the fault plane (Waltham, 1990); b) extensional forced folding (Withjack et al., 1989); c) folding over convex fault bends (Xiao and Suppe, 1992); d) compressional tectonics or inversion (Frost, 1989; rebutted by Badley et al., 1989); e) salt movements (Enachescu, 1988); f) strike-slip (flower) structures; and g) sedimentary structures (Xiao and Suppe, 1992).

All the above mechanisms have difficulty in accounting for one or more of the essential characteristics of the structure from the Sirte Basin described in this paper. For example, in Figure 4 the hanging wall dips increase with depth. This is easily accounted for by a compactional model because of the fact that compaction increases with depth. Mechanisms b), c), d), e) and f) above, in their simplest forms, would produce uniform dips in the hanging wall sediments. Mechanisms a) and f) would predict structures of roughly equal intensity on either side of the fault, whereas the folding of the sediments is observed to be confined to the hanging wall. More detailed arguments against the applicability of some of the mechanisms listed above may be found in Skuce (in press).

The compaction of sediments as they are buried is a process that always occurs and is well documented. This process is also a sufficient mechanism to account for the major structures observed and interpreted on seismic data over the normal fault example shown in Figure 4. Since alternative mechanisms do not account for all the important observed structural features and since there is no other direct evidence that different mechanisms have operated here, it is felt that compaction can confidently be considered the predominant deformation mechanism in this case.

The forward model of compaction structures in Figure 7 shows that subsidence and compaction of the sediments leads to dip changes in the hanging wall horizons. In contrast, subsidence and compaction of the footwall results only in dip changes to the fault, not the horizons, which remain horizontal. Although the magnitude of these particular characteristics of the model are partly dependent on the initial assumptions (horizontal beds, rigid basement, vertical deformation) similar kinds of effects will be seen in most other forward models that incorporate compaction and normal faulting. In particular, beds in the hanging wall of a normal fault can have compaction-induced dips regardless of the footwall lithology. For example, in stage 4 of Figure 7, any assumption of footwall composition would have produced the same geometry; the footwall is not compacted because it has not been buried deeper during stages 1 through 4. This means that identical lithologies and porosities could be present across the fault at stage 4, with the same net amounts of compaction having occurred (but at different times, earlier in the footwall), but compaction structures of the type shown in stage 4 would still have formed. Thus, compaction structures are not necessarily the product of the amount of differential compaction across a fault but, rather, are a result of the different relative timing of the compaction. Since normal faults usually result in increased subsidence of the hanging wall, compaction structures in the hanging wall are to be expected in the majority of cases, even where basement is not involved. Compaction structures will not be seen only in cases where the hanging wall does not subside (i.e., where the footwall is uplifted) and in cases where the hanging wall sediments are uncompactable or precompacted. Structures will also not form in cases where displacements due to compaction are exactly parallel to the fault plane (Waltham, 1990) as opposed to the vertical displacements assumed here.

Fig. 7. Forward model of fault movement, sedimentation and compaction over a planar normal fault. The top of the model is assumed to lie at sea level and at each stage in which sediments are added, the sediments are assumed to completely fill any voids up to sea level. The fault is assumed to be completely planar with a dip of 55°. Thus, no fault-bend folding occurs. Subsidence occurs in two ways (illustrated by arrows): either a generalized vertical subsidence of both hanging and footwalls or by differential subsidence of the hanging wall alone by means of movements across the fault plane. The two periods of fault movement (stages 2, 3 and stage 9) correspond to the rifting stages in the Late Cretaceous and the Eocene, respectively, whereas the generalized subsidence phases (stages 5, 7, 9 and 11) correspond to the Maastrichtian through Oligocene thermal subsidence of the basin (Gumati and Nairn, 1991). The various lithologies assumed for each layer of the model are shown and were chosen to roughly reflect the geology of the study area. The rock properties determine the compaction response of the layers as defined within the GEOSEC software (see text).

Summary/Conclusions

The graben boundary fault between the Agedabia Trough and the Zelten Platform consists of a number of planar fault segments offset by transfer zones. The structural details within the transfer zones are not imaged on the seismic data but certain characteristics can be inferred by comparison with structural models from other areas. The horizons in the hanging wall of the normal fault show a monoclinal structure

with basinward dips up to 20°. This structure formed as a result of the compaction of the sediments above the normal fault. A forward model incorporating fault movement, sedimentation and compaction corroborates this interpretation and demonstrates that compaction alone can be the source of oil-field scale structures in normal fault hanging walls. The model also shows how sedimentary growth can occur within the hanging wall as well as across the fault plane. With the notable exceptions of White et al. (1986) and White and Yielding (1991), compaction has been neglected in most published quantitative structural modelling studies. This neglect has often led to misinterpretations of compaction structures (Skuce, in press).

Compaction anticlines, although not observed in this particular example, can also be formed under certain circumstances; such features could be easily mistaken for inversion structures. Compaction structures will be formed in normal fault hanging walls even where there are no lithology contrasts across the fault. 'Differential compaction' can be, by itself, a sufficient mechanism in causing a compaction structure but it is not a necessary condition. Equally important are the geometric consequences of the burial and compaction of a normal fault hanging wall, regardless of the nature of the footwall. Thus, compaction structures are also consequential in areas of detached listric faulting.

Structural models of the graben boundary fault system described in this paper have helped considerably in the understanding of the deep geology and prospectivity of the area, particularly in regard to the evaluation of fault closures in the hanging wall. The depth to basement, the age and origin of the hanging wall structures, and the likely nature of the faulting within the transfer zones can all be inferred with greater confidence than if the interpretation had been limited to a simple mapping of seismic horizons.

References

Badley, M.E., Rambech Dahl, C. and Agdestein, T., 1988, The structural evolution of the Northern Viking Graben and its bearing on extensional modes of basin formation: J. Geol. Soc. London **145**, 455-472.

_____, _____ and _____, 1989, Discussion on the structural evolution of the Northern Viking Graben and its bearing on extensional modes of basin formation: J. Geol. Soc. London **146**, 1038-1040.

Baldwin, B. and Butler, C.O., 1985, Compaction curves: Bull. Am. Assn. Petr. Geol. **69**, 622-626.

Childs, C., Nicol, A., Walsh, J. and Watterson, J., 1994, Resolution effects in validation of faulted sections: modern developments in structural interpretation, validation and modelling, London: Conference programme with abstracts.

Clifford, H.J., Grund, R. and Musrati, H., 1980, Geology of a stratigraphic giant – the Messlah oilfield, Libya, *in* Halbouty, M.T., Ed., Giant oil and gas fields of the decade 1968-1978: Am. Assn. Petr. Geol., Mem. 36, 507-524.

Enachescu, M.E., 1988, Extended basement beneath the intracratonic rifted basins of the Grand Banks of Newfoundland: Can. J. Expl. Geophys. **24**, 48-65.

Evans, A.C. and Parkinson, D.N., 1983, A half graben and tilted fault block structure in the northern North Sea, *in* Bally, A.W., Ed., Seismic expressions of structural styles: Am. Assn. Petr. Geol., Studies in Geology Series 15, 2.2.2-7-2.2.2-11.

Frost, R.E., 1989, Discussion on the structural evolution of the Northern Viking Graben and its bearing on extensional modes of basin formation: J. Geol. Soc. London **146**, 1035-1038.

Graham, R.H., 1992, Comparison of the Tethyan margin of the SW Alps with the North Sea: Am. Assn. Petr. Geol., Field Trip Handbook, Alpine Mesozoic Basin in the SE of France (unpublished).

Gray, R.J. and Roberts, D.C., 1984, A seismic model of faults in the Cooper Basin: Austral. Petr. Expl. Assn. J. **24-1**, 421-428.

Gumati, Y.D. and Nairn, A.E.M., 1991, Tectonic subsidence of the Sirte Basin, Libya: J. Petr. Geol. **14**, 93-102.

Jackson, J.A., 1987, Active normal faulting and crustal extension, *in* Coward, M.P., Dewey, J.F. and Hancock, P.L., Eds., Continental extensional tectonics: Geol. Soc., Spec. Publ. 28, 3-17.

Kusznir, N.J., Marsden, G. and Egan, S.S., 1991, A flexural-cantilever, simple-shear/pure-shear model of continental lithosphere extension: applications to the Jeanne d'Arc Basin, Grand Banks and Viking Graben, North Sea, *in* Roberts A.M., Yielding, G. and Freeman, B., Eds., The geometry of normal faults: Geol. Soc., Spec. Publ. 56, 41-60.

Milton, N.J., Bertram, G.T. and Vann, I.R., 1990, Early Palaeogene tectonics and sedimentation in the central North Sea, *in* Hardman, R.F.P. and Brooks, J., Eds., Tectonic events responsible for Britain's oil and gas reserves: Geol. Soc., Spec. Publ. 55, 339-351.

Morley, C.K., 1994, Discussion of potential errors in fault heave methods for extension estimates in rifts, with particular reference to fractal fault populations and inherited fabrics: modern developments in structural interpretation, validation and modelling, London: Conference programme with abstracts.

_____, Nelson, R.A., Patton, T.L. and Munn, S.G., 1990, Transfer zones in the East African rift system and their relevance to hydrocarbon exploration in rifts: Bull. Am. Assn. Petr. Geol. **74**, 1234-1253.

Peacock, D.C.P. and Sanderson, D.J., 1994, Geometry and development of relay ramps in normal fault systems: Bull. Am. Assn. Petr. Geol. **78**, 147-165.

Skuce, A.G., in press, Forward modelling of compaction above normal faults: an example from the Sirte Basin, Libya, *in* Buchanan, P.G. and Nieuwland, D.A., Eds., Modern developments in structural interpretation, validation and modelling: Geol. Soc., Spec. Publ.

Terry, R.C. and Williams, J.J., 1969, The Intisar 'A' bioherm and oil field, Sirte Basin, Libya - its commercial development, regional Paleocene geologic setting and stratigraphy: The Institute of Petroleum, Great Britain, 31-48 (reprinted from The exploration for petroleum in Europe and North Africa).

Waltham, D., 1990, Finite difference modelling of sand box analogues, compaction and detachment free deformation: J. Struct. Geol. **12**, 375-381.

Westaway, R. and Kusznir, N.J., 1993, Fault and bed rotation during continental extension: block rotation or vertical shear?: J. Struct. Geol. **15**, 753-770.

White, N.J., Jackson, J.A. and McKenzie, D.P., 1986, The relationship between the geometry of normal faults and that of the sedimentary layers in their hanging walls: J. Struct. Geol. **8**, 879-909.

_____ and Yielding, G., 1991, Calculating normal fault geometries at depth: theory and examples, *in* Roberts, A.H., Yielding, G. and Freeman, B., Eds., The geometry of normal faults: Geol. Soc., Spec. Publ. 56, 251-260.

Withjack, M.O., Meisling, K.E. and Russell, L.R., 1989, Forced folding and basement-detached normal faulting in the Haltenbanken area, offshore Norway, *in* Tankard, A.J. and Balkwill, H.R., Eds., Extensional tectonics and stratigraphy of the North Atlantic margins: Am. Assn. Petr. Geol., Mem. 46, 567-575.

Xiao, H. and Suppe, J., 1992, Origin of rollover: Bull. Am. Assn. Petr. Geol. **76**, 509-529.